Airborne Ku-Band Polarimetric Radar Remote Sensing of Terrestrial Snow Cover

Simon H. Yueh, *Fellow, IEEE*, Steve J. Dinardo, Ahmed Akgiray, Richard West, Donald W. Cline, and Kelly Elder

***Abstract*—Characteristics of the Ku-band polarimetric scatterometer (POLSCAT) data acquired from five sets of aircraft flights in the winter months of 2006–2008 for the second Cold Land Processes Experiment (CLPX-II) in Colorado are described in this paper. The data showed the response of the Ku-band radar echoes to snowpack changes for various types of background vegetation in the study site in north central Colorado. We observed about 0.15–0.5-dB increases in backscatter for every 1 cm of snow-water-equivalent (SWE) accumulation for areas with short vegetation (sagebrush and pasture). The region with the smaller amount of biomass, signified by the backscatter in November, seemed to have the stronger backscatter response to SWE in decibels. The data also showed the impact of surface hoar growth and freeze/thaw cycles, which created large snow-grain sizes, ice crust layers, and ice lenses and consequently increased the radar signals by a few decibels. The copolarized HH/VV backscatter ratio seems to indicate double-bounce scattering between the ground surface and snow or vegetation. The cross-polarized backscatter [vertical–horizontal (VH)] showed not only the influence of vegetation but also the strong response to snow accumulation. The observed HV/VV ratio suggests the importance of multiple scattering or nonspherical scattering geometry of snow grain in the dense-media radiative transfer scattering model. Comparison of the POLSCAT and QuikSCAT data was made and confirmed the effects of mixed terrain covers in the coarse-resolution QuikSCAT data.**

***Index Terms*—Microwave remote sensing, radar, snow.**

I. Introduction

FRESH water stored in snow on land is an important component of the global water cycle. In many regions of the world, it is vital to health and commerce. High-resolution snow-water-equivalent (SWE) observation requirements were articulated by the Global Earth Observing System of Systems, the Integrated Global Observing Strategy, and World Meteorological Organization/World Climate Research Programme Climate and Cryosphere Project Science and Co-ordination Plan. In 2005, the Cold Regions Hydrology High-resolution Observatory ($CoReH_2O$) proposal concept based on X- and Ku-band synthetic-aperture-radar (SAR) technologies was submitted by the international cold land processes science community to the European Space Agency and was selected for an 18-month study for space implementation [1]. In addition, the Snow and Cold Land Processes mission, also based on the dual-frequency SAR concept, was one of the satellite missions recommended for future NASA implementations in the recent earth science decadal study report [2].

In past studies, ground-based microwave radar measurements at 5–35-GHz frequencies were obtained for snow with different wetness, depth, and SWE [3]–[9]. These historic measurements demonstrated the microwave radar response to snowpack for limited and/or artificial snow conditions. However, the impact of various vegetation covers, nominally present in the natural environment, has not yet been explored.

Demonstration of spaceborne SAR observations for SWE measurements was first report in [10] and [11]. The three-frequency (L-, C-, and X-band) multipolarization radar backscatter data from the Shuttle Imaging Radar-C (SIR-C) mission were used to estimate snow density, depth, and particle size. The physical-model-based retrieval approach provided reasonable estimates of SWE in comparison with *in situ* measurements. However, the retrieval uncertainty remained fairly large, probably because of the relatively smaller response of SIR-C frequencies to SWE than higher microwave frequencies. More recent modeling research [12], [13] indicated that dual frequencies at combination of X- and Ku-bands are more optimal for remote sensing of SWE.

Recent analyses of spaceborne QuikSCAT scatterometer data with footprint size on the order of 30 km have suggested the presence of snowpack information in Ku-band radar observations for complex terrain [14], [15]. The matchup of the QuikSCAT data with the National Snow Analysis (NSA) on a nominal daily basis was performed by the National Operational Hydrologic Remote Sensing Center, National Weather Service, National Oceanic and Atmospheric Administration, for the data acquired from July 2003 to April 2004 for several target sites, including the Mammoth Pass in California and three sites in Colorado. These target locations all have mountainous landscapes with a large percentage of forest stands. The QuikSCAT and NSA SWE scatter plots for all of the targeted areas indicate a monotonic increase of radar echo level for increasing SWE. In general, the change is about 1 dB in backscatter for 10-cm change of SWE for all of these areas. However, it remains unclear how the effects of mixed terrain cover in coarse-resolution

Manuscript received August 6, 2008; revised January 8, 2009 and January 30, 2009. First published August 18, 2009; current version published September 29, 2009.

S. H. Yueh, S. J. Dinardo, A. Akgiray, and R. West are with the Jet Propulsion Laboratory, California Institute of Technology, Pasadena, CA 91109-8099 USA (e-mail: syueh@jpl.nasa.gov; Steve.Dinardo@jpl.nasa.gov; Ahmed.Akgiray@jpl.nasa.gov; richard.west@jpl.nasa.gov).

D. W. Cline is with the National Operational Hydrologic Remote Sensing Center, National Weather Service, National Oceanic and Atmospheric Administration, Chanhassen, MN 55317-8580 USA (e-mail: Donald.Cline@noaa.gov).

K. Elder is with the Rocky Mountain Research Station, U.S. Department of Agriculture Forest Service, Fort Collins, CO 80526-2098 USA (e-mail: kelder@fs.fed.us).

Color versions of one or more of the figures in this paper are available online at http://ieeexplore.ieee.org.

Digital Object Identifier 10.1109/TGRS.2009.2022945

TABLE I
CLPX-II POLSCAT FLIGHT SUMMARY IN COLORADO

Campaign	Year	Date	General Snowpack conditions
IOP1	2006	December 2, 3, 4, 5	Dry snowpack
IOP2	2007	January 25, 26, 28, 29	Dry snowpack
IOP3	2007	February 22, 23	Melting snow pack over the day time and refrozen over night
Background survey	2007	November 8, 9	No snow, except in the Park Range and Medicine Bow Mountains
Repeatability test	2008	March 10	Snow over all sites.

TABLE II
KEY POLSCAT CHARACTERISTICS

Frequency	13.9 GHz
Polarization	VV, HH, HV, and VH
Antenna Beam width	3 degrees
Incidence Angle	Commandable in flight from 0 to 65 deg
Azimuth Angle	Commandable from 0 to 360 degrees
Footprint resolution at 5000 ft above ground level	100 m (azimuth) and 120 m (range) at 35 degree incidence
Noise Equivalent Sigma0	<-40 dB
Calibration stability	<0.1 dB

QuikSCAT measurements have influenced the radar response to snow accumulation.

Within the U.S., the cold land processes research community has supported the second Cold Land Processes Experiment (CLPX-II) during the 2006–2008 winter seasons in Colorado and winter 2007–2008 in Alaska [16]. The objective of the CLPX-II experiment is to acquire an extensive Ku-band radar backscatter from various types of snow and vegetation cover, together with extensive *in situ* snow measurements. The experiment will serve as a testbed, providing the data set for the development of snow water retrieval algorithms and to test radiative transfer models [17], [20] for a variety of snowpacks. This paper describes the characteristics of the POLSCAT data from the CLPX-II in Colorado and sensitivity of Ku-band multipolarization radar response to SWE.

II. POLSCAT/CLPX-II

From December 2006 to March 2008, we deployed the Ku-band polarimetric scatterometer (POLSCAT) built by the Jet Propulsion Laboratory for five sets of aircraft flights (Table I) in north central Colorado. POLSCAT includes two-axis gimbals for a conically scanning parabolic antenna at a constant elevation angle, which is controllable from 0° (nadir) to 65°. POLSCAT transmits at a pulse repetition interval (PRI) of 350 μs with alternating vertical (V) and horizontal (H) polarizations from pulse to pulse. For each transmit pulse, POLSCAT detects the V- and H-polarization echoes simultaneously through two parallel receivers. This transmit and receive design results in four polarization combinations, namely, VV, HV, HH, and VH, for the detected radar echoes. The first letter of each polarization combination denotes the receive polarization, and the second letter denotes the transmit polarization. More detailed characteristics of the POLSCAT electronics, including the calibration loop for transmit power and receiver gain calibration, can be found in [18], with the key characteristics being summarized in Table II. For the flight campaigns, we installed POLSCAT on a Twin Otter aircraft and operated the antenna at 35° elevation angle (Fig. 1). A set of Twin Otter flights were also conducted at 45° elevation angle to acquire data for cross-calibration with the QuikSCAT data.

Three intensive observing periods (IOPs) with a total of ten aircraft flights were completed in December 2006 (IOP1), January 2007 (IOP2), and February 2007 (IOP3). These three IOPs were conducted with intensive sampling in many locations. In addition, we performed three flights in November 2007 and March 2008 to extend the time series. The first two flights were conducted in early November 2007 to survey the radar response of the study site before appreciable snow accumulation (Table I). One additional data flight was completed on March 10, 2008, for late-winter conditions after the snowpack went through some freeze–thaw cycles from February to March. Because the *in situ* sampling equipment was committed to the CLPX-II campaign in Alaska from late November 2007 to February 2008, we could not complete *in situ* sampling for these three flights in November 2007 and March 2008. However, the data from these three flights, together with the data from three IOPs, allow us to explore the temporal changes of radar response to snow conditions from late autumn to early spring.

Each flight imaged an area of 9 km wide × 90 km long (Fig. 2) from the Quarry and Thorpe Mountains on the west to the Medicine Bow Mountains on the east. The Park Range (approximately 12 000 ft in elevation) is a mountain range of the Rocky Mountains in north central Colorado, separating the watersheds of the Yampa River and Oak Creek from North Park, which is a sparsely populated basin (about 8800 ft in elevation) between the Park Range and Medicine Bow Mountains. North Park encompasses several smaller tributaries, including the Michigan River and Illinois River. Located to the east of the Owl Mountain is the valley of the Michigan River. On the west side of the Owl Mountain is the Illinois River watershed, where the city of Rand is located. South of North Park is the Rabbit Ears Range (approximately 11 000 ft in elevation), stretching east–west along on the continental divide, which includes several mountains, such as Ironclad Mountain, Spicer Peak, and Buffalo Peak (Fig. 2). This study area consisted of a variety of land-use/land-cover characteristics, including coniferous and deciduous forests, sagebrush, and pasture fields. The primary economic activities in North Park are cattle ranching and timber harvesting. In the watersheds of the Yampa River and Oak

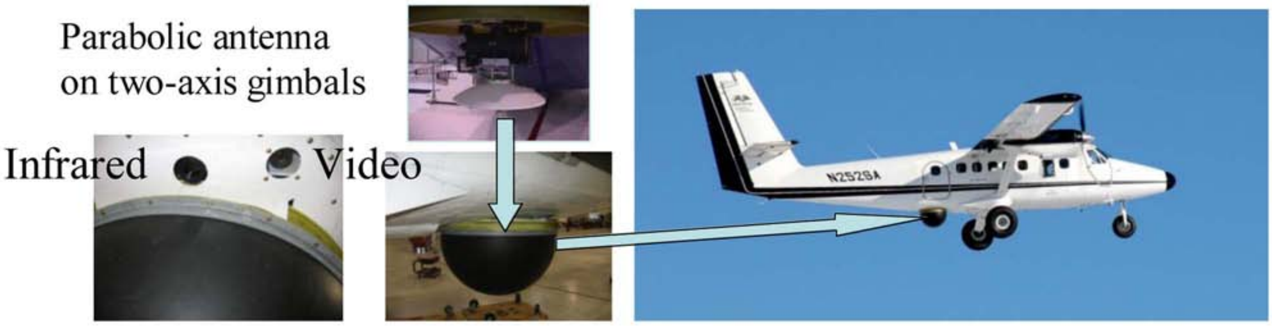

Fig. 1. POLSCAT on the Twin Otter with two-axis gimbals for the conical scanning of the parabolic antenna at any incidence angle from 0° to 65°. There are nadir-looking infrared and video cameras mounted adjacent to the POLSCAT antenna radome.

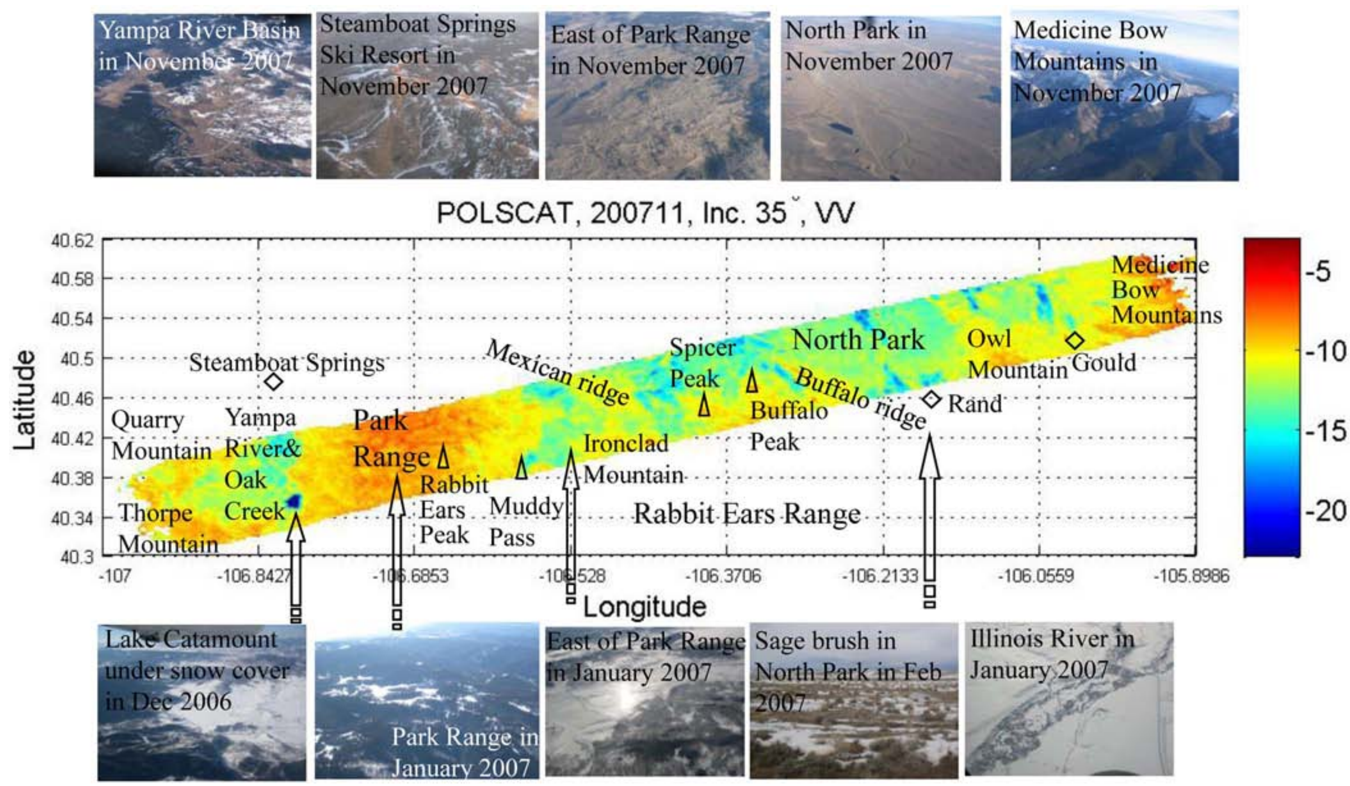

Fig. 2. Test site is about 90 km long from west to east and 9 km wide from south to north. The middle panel shows the color-coded POLSCAT VV radar data in decibels, acquired in December 2006. The upper line of images shows the selected areas in fall with little snow cover, while the lower line of images shows similar areas in winter with extensive snow cover.

Creek, surrounded by the Quarry Mountain, Thorpe Mountain, and Park Range, there are also ranches with irrigated grass pasture fields. Just located at the foothills of the Park Range is the Catamount Lake, where snow and ice cover are nominally present from December to March. In the Park Range and the Rabbit Ears Range is the Routt National Forest with mostly coniferous forests, meadows, and some deciduous trees at lower elevation.

The Twin Otter flight altitude was maintained at about 14 000 ft above sea level, resulting in the above ground level of approximately 4000–7000 ft over the study area. At this altitude, the POLSCAT swath width for conical scanning at 35° elevation angle is about 1.7–3.4 km, depending on the ground elevation. For each flight, we flew the POLSCAT on the Twin Otter with six parallel flight tracks, approximately equally spaced to achieve complete coverage of the entire 9 km × 90 km area.

During the background survey flights in November 2007, the visual surveillance (photographs and operator observations) from the Twin Otter aircraft and a road trip survey on the ground indicated no snow cover in North Park (Fig. 2). There was patchy and thin snow cover in the Park Range and the watersheds of the Yampa River and Oak Creek. The Steamboat Springs Ski resort was almost bare with some snow in the trails (the second photograph on the top from the left in Fig. 2). The Park Range had more snow than the Yampa River basin although likely less than a few-centimeter SWE on average. The background survey flight data provided a useful reference data set for assessing the influence of snow accumulation on the radar backscatter over the study area.

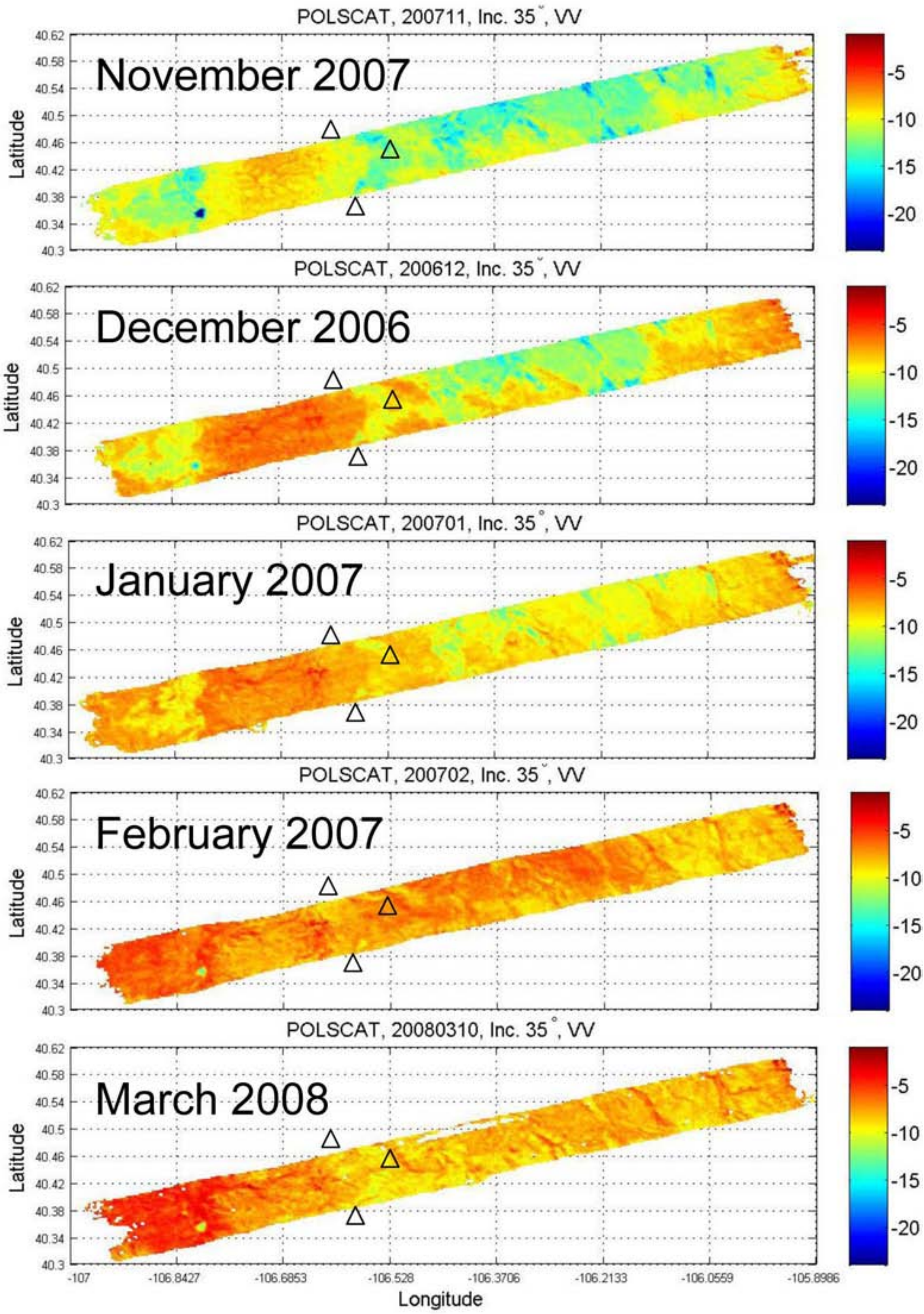

Fig. 3. POLSCAT VV radar images from top to bottom are for November 8–9, 2007 (background survey), December 2–5, 2006 (IOP1), January 25–29, 2007 (IOP2), February 22–23, 2007 (IOP3), and March 10, 2008. The VV data are color coded, with the color key in decibels shown in the color bar. The three small triangles mark a triangular area of deciduous forest with lower backscatter than other coniferous forest areas.

To provide calibration reference for POLSCAT, we flew the Twin Otter over the National Data Buoy Center (NDBC) buoy 46022 on March 4, 2008, when the aircraft was returning to Colorado from Alaska. The NDBC buoy 46022 is located off the northern California coast, about 17 nmi west–southwest of Eureka, California. We performed four passes over the buoy with the POLSCAT operating at about 45° incidence angle, corresponding to the incidence angle of the inner beam of the QuikSCAT scatterometer. The passes were completed in 1 h, during which the ocean surface wind speed was in the range of 9.5–10.2 m/s based on the buoy data acquired at every 10 min. We estimated the expected radar backscattering coefficient (σ_0) from the QuikSCAT model function [23] using the buoy wind speed and direction. The POLSCAT radiometric calibration was adjusted to match the POLSCAT data and QuikSCAT model estimates. The same radiometric calibration coefficient was used to process all the POLSCAT/CLPX-II data to achieve relative calibration consistency for the data from all IOPs.

TABLE III
BACKSCATTER FROM LAKE CATAMOUNT

	VV (dB)	HH (dB)	HV (dB)
8-9 November 2007	-43.1	-46.5	-48.3
2-5 December 2006	-16.1	-15.2	-24.9
25-29 January 2007	-9.4	-8.5	-17.9
22-23 February 2007	-12.2	-11.9	-21.4
10 March 2008	-10.1	-10.1	-19.1

III. DATA CHARACTERISTICS

The POLSCAT data were binned and averaged on 200-m grids for each observation period (Table I). The VV radar image for the data acquired on November 8 and 9, 2007 (top panel in Fig. 3), shows distinct backscatter levels for different terrain covers. The backscatter from the forests in the Routt National Forest (Park Range and Rabbit Ears Range), Owl Mountain, and Medicine Bow Mountains showed strong radar backscatters of about -5 to -10 dB (yellow to orange colors). Inside the triangular region with the corners marked by three small triangles are deciduous forests with lower backscatter (green–yellow color) than the coniferous forests in the Park Range (orange color in Fig. 3). The areas with sagebrush cover or grass pasture in North Park and the Yampa River/Oak Creek watersheds had weaker backscatters of about -10 to -15 dB (green to light blue colors).

In November 2007, the weakest backscatter (deep blue) came from Lake Catamount, several lakes, and the riverbeds of Illinois River and Michigan River in North Park. The VV and HH backscatters from Lake Catamount were as low as -40 dB, indicating minimum wind-induced ripples or waves on the water surface. The cross-polarized backscatter, HV, from Lake Catamount was less than -43 dB, which supports our assessment of the POLSCAT system noise floor (Table II). When there were snow and ice present in the lake from December to March, the radar backscatter could increase significantly to about -10 dB for VV and HH polarizations (Table III). The snow and ice apparently were also strong depolarized scattering sources, resulting in about -20 dB for HV response.

Comparison of the VV data from three IOP campaigns (the middle three panels in Fig. 3) and the November 2007 data (top panel) shows the impact of snowpack on Ku-band radar backscatter over time. The December 2006 radar backscatter was about 1–3 dB (top panel in Fig. 4) stronger than the November 2007 data across the entire study site, including the forested areas in the Routt National Forest and the Medicine Bow Mountains. From IOP1 (December 2–5, 2006) to IOP2 (January 25–29, 2007), the radar backscatter showed further increase by about 2–3 dB over the sagebrush and grass pasture areas in North Park and the Yampa River/Oak Creek watersheds (middle panel in Fig. 4). From IOP2 to IOP3 (February 22–23, 2007), the sagebrush and pasture fields had dramatic VV increases of about 3–5 dB (lower panel in Fig. 4).

Interestingly, the radar backscatter of the snow-covered sagebrush and pastures in the Yampa River/Oak Creek watersheds and North Park exceeded or became comparable with the backscatter from the forested areas in the Park Range in February and remained significant in March 2008 (bottom panel in Fig. 3). Examination of *in situ* observations indicated that there was widespread depth hoar in the snowpack in late February. Ice lenses were also present, which were caused by several melting and refreezing events starting in early February. The large snow grains in the depth hoar and the ice lenses were apparently the cause of the significant increase in radar backscatter after January.

Another intriguing characteristic is the initial rise, followed by a drop in the radar backscatter from the coniferous forests in the Park Range, Owl Mountain, etc., over time (Fig. 4). The top panel in Fig. 4 shows that the radar backscatter of coniferous forests in December 2006 was about 2–3 dB stronger than that in November 2007, while the change reduced to about 1–2 dB in January 2007 (middle panel) and about a few tenths to 1 dB in February (bottom panel). This should be contrasted with the increasing backscatter in the areas with short and sparse vegetation cover. It is unclear why the radar backscatter should decrease by about 2 dB from December to February for coniferous forests. One hypothesis is that the water content of the needle leaves and stems of coniferous trees decreased gradually over winter. Reduced water content will lower the dielectric constant of the tree canopies and, hence, the radar backscatter. Because no dielectric constant measurements were made, we cannot confirm or reject this hypothesis. The phenomenon of decreasing backscatter from coniferous forests after December should be a subject for further research.

The signals for cross-polarization, i.e., HV or VH, had similar features and distinct characteristics (Figs. 5 and 6). The cross-polarized (HV) radar backscatter shown in Fig. 5 had strikingly similar spatial distribution and temporal change to the VV backscatter shown in Fig. 3. However, there seemed to be a sharper contrast in the HV backscatter between forested areas and sage brush or pasture fields in November, December, and January (top three panels in Fig. 5). For example, the VV backscatter image has more fuzzy transition from strong (orange color) to moderate (green color) amplitude, just to the east of the Park Range, while the HV backscatter image has shown sharper transition. This indicates that the HV backscatter carries more distinct information about the vegetation types than the VV or HH backscatter.

Another distinct characteristic is the significant strength of the HV backscatter from the snowpack. In November 2007 when there was no snow, the HV backscatter in the Yampa River/Oak Creek watersheds was about -15 to -20 dB and less than -20 dB in North Park. Toward the end of winter in March 2008, the HV backscatter in the Yampa River/Oak Creek watersheds reached as high as -10 to -15 dB, which is comparable to the backscatter from the forested areas in the Routt National Forest. It was suggested in [17] that the strong cross-polarized backscatter was the result of multiple scattering between densely packed sticky spheres (snow grains). An alternate source of the strong HV backscatter is the nonspherical geometry of snow grains, which will introduce cross-polarized radar energy into the backscatter direction. Our data set confirms the significant magnitude of the HV backscatter, which

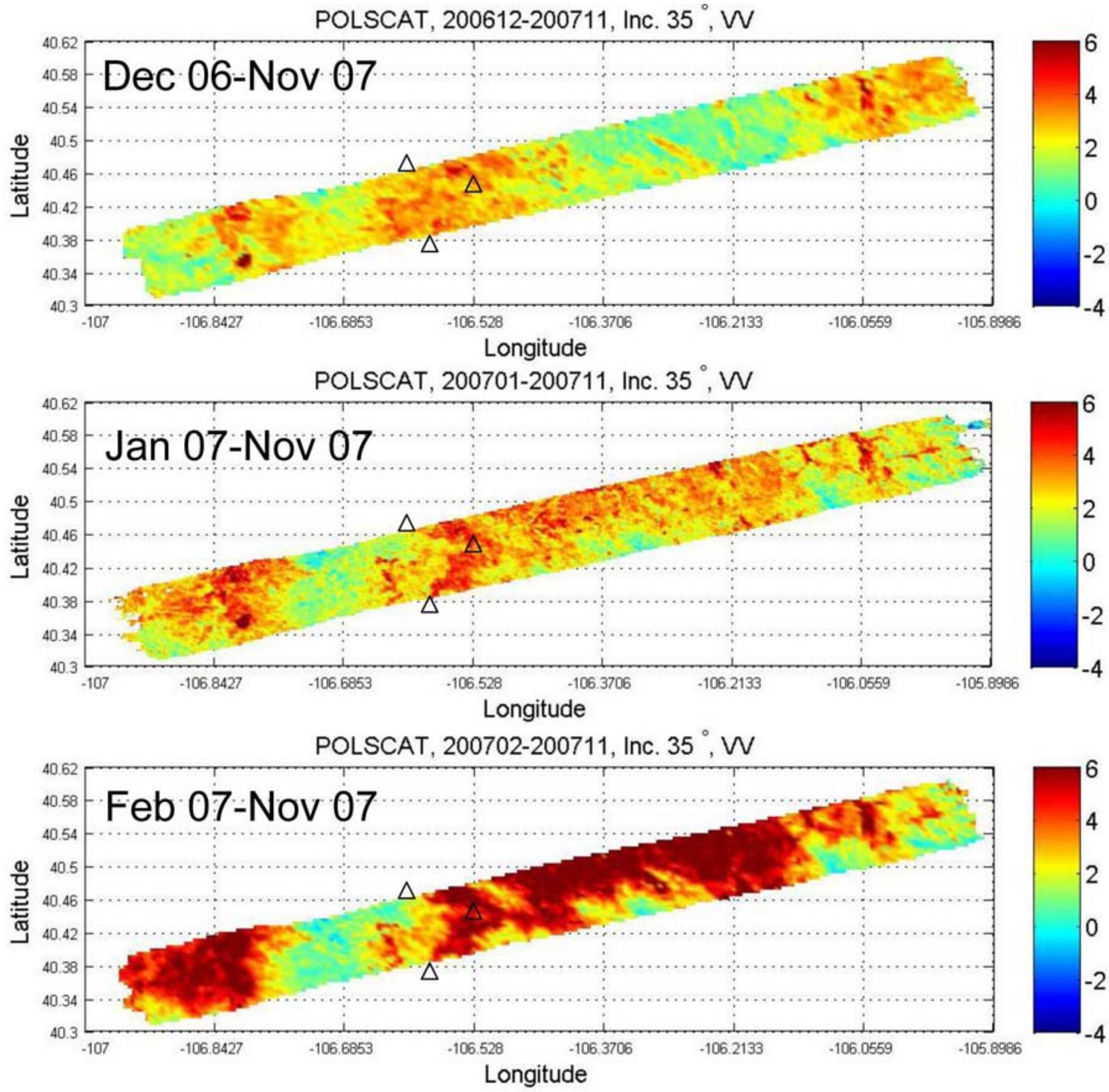

Fig. 4. Panels show the changes of POLSCAT VV backscatter with respect to the data acquired in November 2007. The changes are color coded in decibels.

can be caused by nonspherical snow grains and/or multiple scattering between snow grains [17].

It appeared that, by comparing the top two panels in Figs. 4 and 6, the HV backscatter changed less than the VV backscatter over time in some regions in North Park as the snow accumulated in December and January (see also Section IV for the discussion of the curve for North Park in Fig. 11). For example, the backscatter difference between December 2006 and November 2007 for the deciduous forests within the triangular region was about 3 dB for VV and 2 dB for HV. Also, the backscatter change between January and November 2007 was more apparent in VV than in HV over North Park with sagebrush cover. One possible interpretation is based on the relative volume scattering contributions of snow and vegetation. Supposedly, let us approximate the total radar backscatter as the sum of backscatter from vegetation and snow. If the vegetation and snow volume scattering ratio is larger for HV than for VV, it will require more change in the HV scattering from the snow to raise the total backscatter in decibels for HV. In other words, the scattering contribution from vegetation may cause the total HV backscatter in decibels to be less sensitive to snow accumulation. Our results suggest future research concerning electromagnetic scattering modeling of mixed snow–vegetation medium to provide detailed consistent interpretation of our observations.

Just to the west of the triangular region is an open meadow in the Park Range, roughly centered at latitude 40.38° N and longitude 106.64° W, where the change of radar backscatter was stronger than that of the neighboring areas with coniferous or deciduous trees (Fig. 6). The HV backscatter change from November 2007 was about 3–4 dB in January 2007 and 5–6 dB in February 2007. Similar changes can be seen in Fig. 4 for the VV backscatter. The fact that the radar backscatter in the open meadow surrounded by forests increased in time indicates the significant impact of snow accumulation on the radar observations. In this open meadow, we selected four sites for intensive *in situ* sampling and found that the snow depth of this open meadow could reach about 1 m, which is much larger than the snow depth of about 10–30 cm or less in North Park. The POLSCAT observations of backscatter changes support the

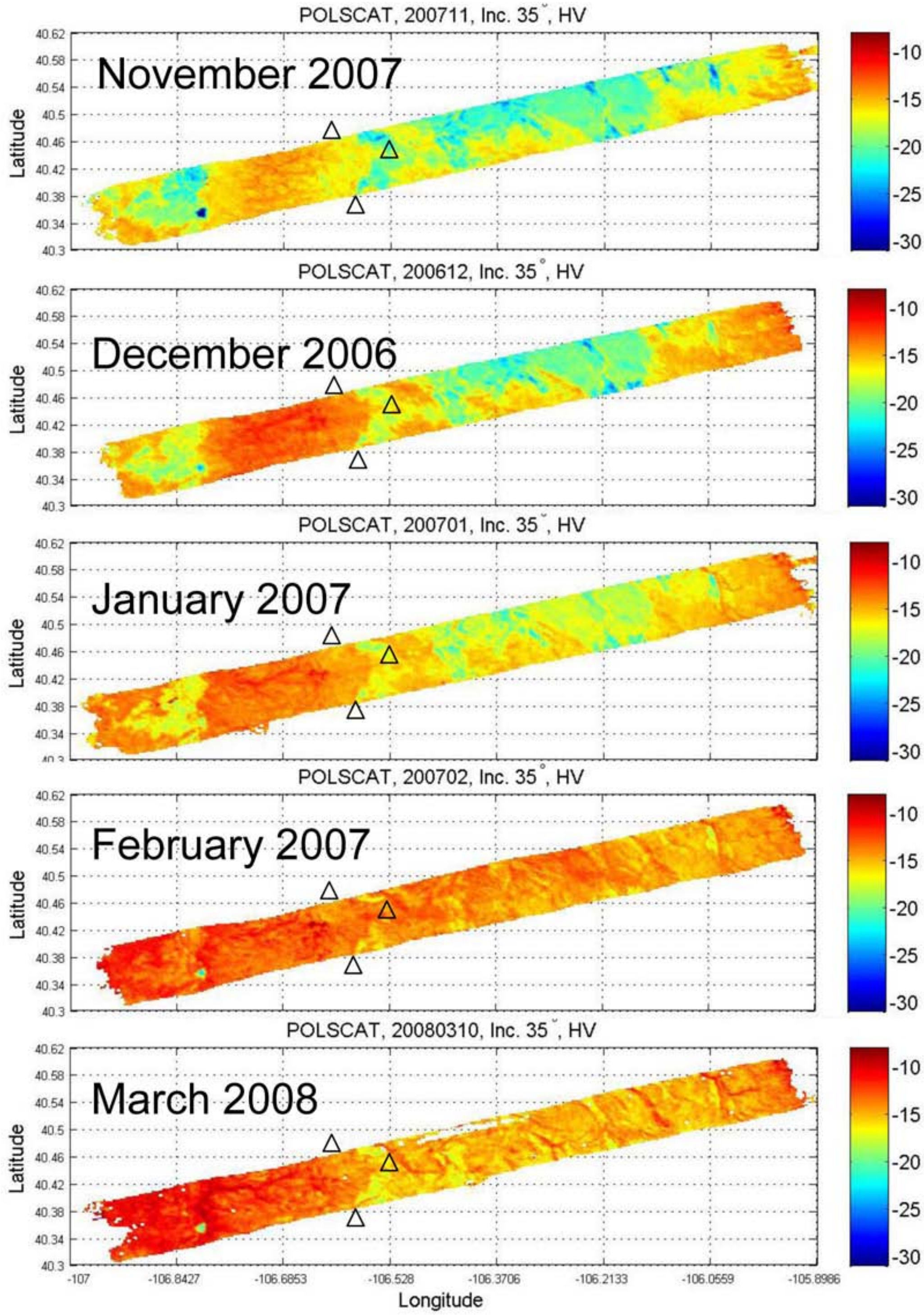

Fig. 5. POLSCAT HV radar images from top to bottom are for November 8–9, 2007 (background survey), December 2–5, 2006 (IOP1), January 25–29, 2007 (IOP2), February 22–23, 2007 (IOP3), and March 10, 2008. The HV data are color coded, with the color key in decibels shown in the color bar.

feasibility of snow remote sensing for snowpack with moderate depth.

The ratio of copolarized radar backscatter (VV and HH) also indicates distinct characteristics of snow cover and vegetation. Although the levels of HH and VV backscatter data were quite close to each other, the ratio did have systematic changes over months (Fig. 7). In November 2007, the HH/VV ratio is quite uniform within a few tenths of decibels, except for a few areas where the ratio can reach quite significant levels (orange color). For example, the riverbed of the Illinois River near the west of latitude 40.54° N and longitude −106.2133° W in North Park had greater HH backscatter than VV backscatter by about 1 dB (red color in Fig. 7). There are four mechanisms nominally considered for the microwave scattering modeling of snowpack or vegetation (Fig. 8). For ground-surface scattering, there are two surface scattering models, including

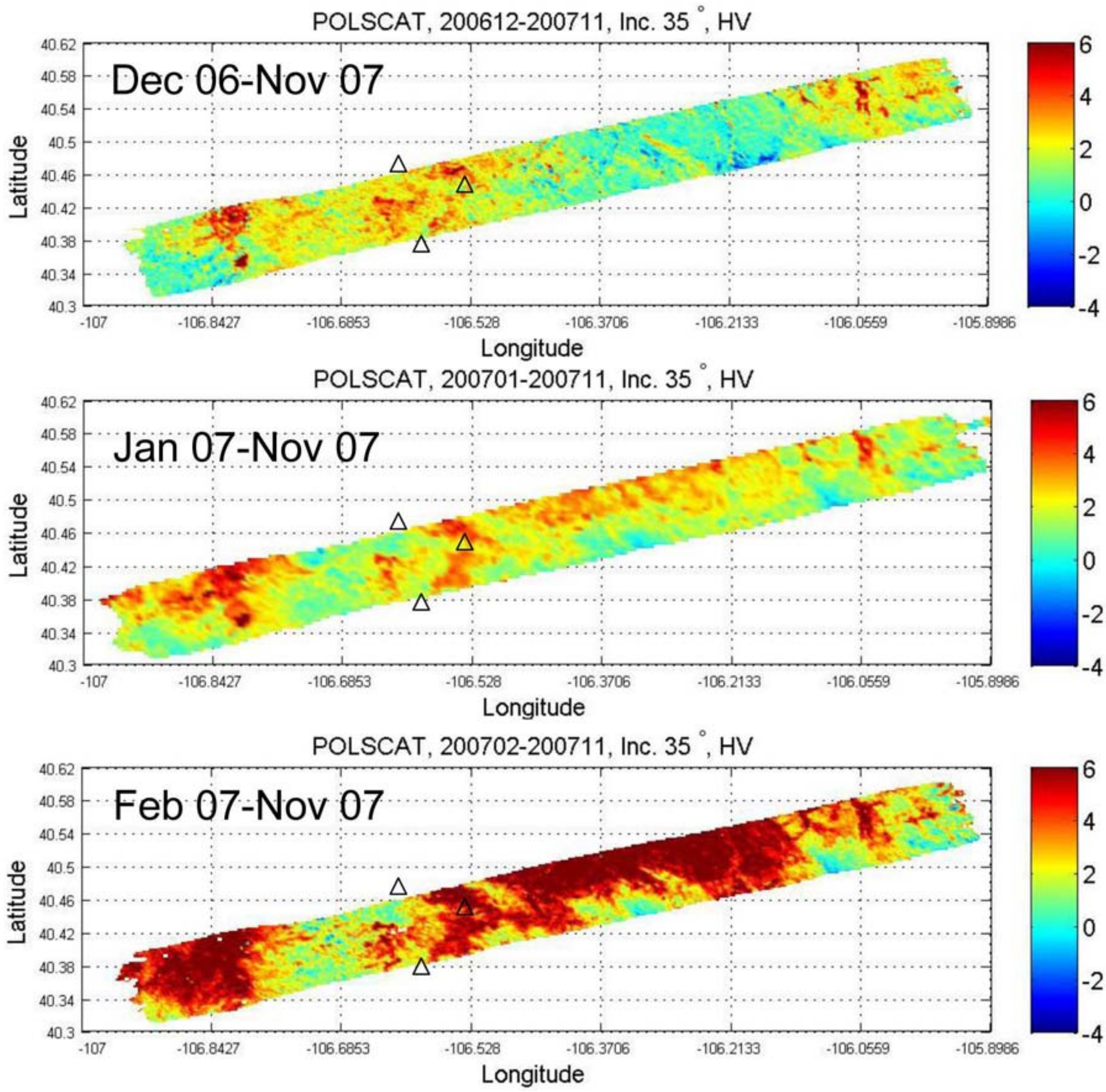

Fig. 6. Panels show the POLSCAT HV backscatter changes with respect to the data acquired in November 2007. The changes are color coded in decibels.

the geometric optic (GO) and Bragg scattering, nominally applied to the interpretation of remote sensing data. The GO surface scattering model, which is applicable to surfaces with large and gentle variations in surface slopes, will result in unity HH/VV ratio, while the Bragg scattering model, which is applicable to surfaces with small root-mean-square (rms) roughness, will lead to the HH/VV ratio of less than unity (or 0 dB). Therefore, the observed HH/VV ratio in many regions, where it was greater than unity in November, is not the result of either Bragg or GO scattering by rough surfaces.

Two scattering mechanisms may contribute to the observed HH/VV ratio over the study site in November. One is the volume scattering from vegetation, which may have more horizontally oriented leaves, twigs, or branches. If the vegetation components have preferred H orientation, the radar scattering effects may be more effective for H polarization. However, it seems unlikely for all types of vegetation in the study site, including pasture, coniferous tress, deciduous trees, and sagebrush to have preferred H orientation.

The other mechanism is the double-scattering effect by the ground and vegetation (mechanisms 3 and 4 in Fig. 8). The radar transmit signals can be bounced off the ground and then scattered by the vegetation toward the radar and vice versa. Because the Fresnel reflection coefficient for H polarization (R_h) for soil (dielectric) surfaces is larger than that for V polarization (R_v), the double-bounce (volume and surface) scattering effects will result in stronger HH backscatter than VV backscatter.

Table IV provides the nominal dielectric constant of dry soil, dry snow, and ice. The dielectric constant of the dry snow in Table IV is evaluated using the following empirical formula [22]:

$$\varepsilon = 1 + 1.6\rho + 1.86\rho^2. \tag{1}$$

Here, ρ is the snow density in grams per cubic centimeter. From the *in situ* measurements in December 2006 and January 2007, the snow density was mostly in the range of

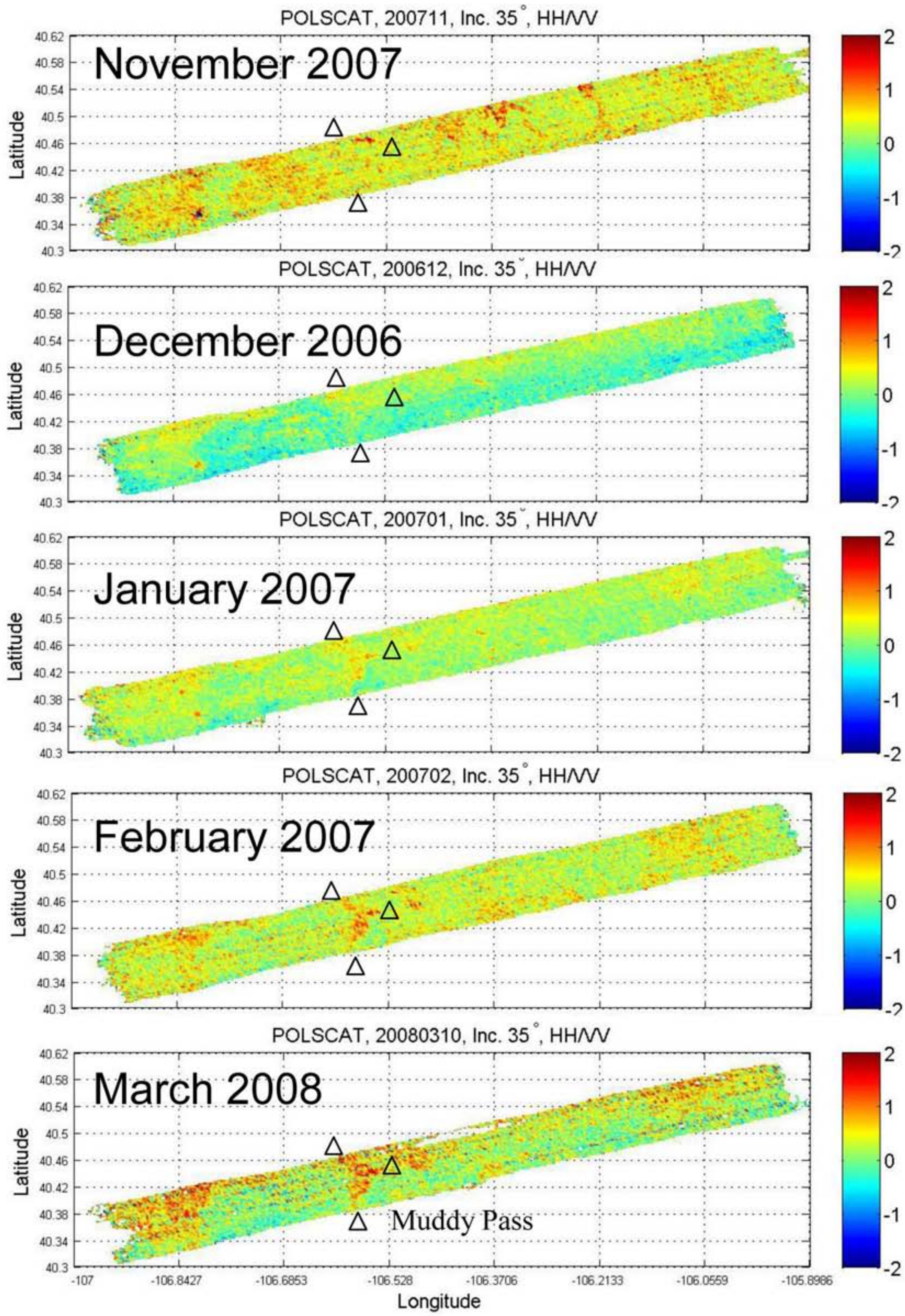

Fig. 7. POLSCAT HH/VV backscatter ratio images from top to bottom are for November 8–9, 2007 (background survey), December 2–5, 2006 (IOP1), January 25–29, 2007 (IOP2), February 22–23, 2007 (IOP3), and March 10, 2008. The HH/VV ratios are color coded, with the color key in decibels shown in the color bar.

0.1–0.3, and the resulting dielectric constant for dry snow is approximately between 1.3 and 1.5. Table V provides the square of Fresnel reflection coefficients for the snow density of 0.3 for several surface combinations at 35° incidence angle. For bare-soil surface (air above soil), about 7.5% of horizontally polarized incidence energy is reflected at 35° incidence angle, which is more significant than the 2.4% reflection for V polarization. When there is a dry-snow layer above the soil surface,

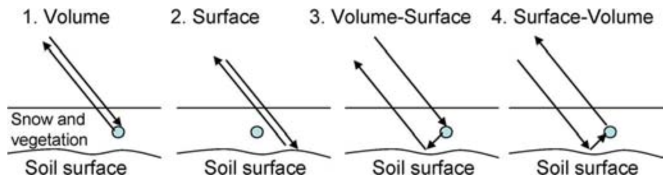

Fig. 8. Four mechanisms for radar backscattering from snowpack. (1) Volume scattering from snow grains or vegetation. (2) Surface scattering from the snow–ground interface. (3) Scattering by volume scatterers and reflection by the surface. (4) Reflection by the ground surface and then scattering by volume scatterers.

TABLE IV
NOMINAL RELATIVE DIELECTRIC CONSTANT OF SNOW, ICE, AND SOIL

Air	1
Snow (0.2 g/cm^3 to 0.3g/cm^3)	1.44 to 1.57
Ice	3.5
Sandy soil	2.5
Dry loamy soil	2.4
Dry clay soil	2.2

the reflected power reduces to 2% for H polarization and 0.8% for V polarization.

We now consider a rough estimation for the double-bounce effects on the HH/VV ratio. For relatively smooth surface, the radar backscatter contributed by the four terms shown in Fig. 8 can be approximated as

$$\sigma_0 \cong \sigma_{0\mathrm{surface}} + \sigma_1 + \alpha |R|^2 \sigma_2. \tag{2}$$

Here $\sigma_{0\mathrm{surface}}$ represents the surface scattering, σ_1 corresponds to the volume scattering from direct backscatter (vegetation and snow), and σ_2 corresponds to the bistatic scattering of the volume scatterers. The ground reflection effect is modeled by the Fresnel reflection coefficient R. The factor (α) accounts for the effects of reciprocal paths (3 and 4 in Fig. 8). In principle, the scattered electric fields from these two reciprocal paths interact coherently, and hence, factor α is four. Also, to be more general, the last term should be averaged over the slope distribution of the ground surface. Note that the aforementioned equation is only valid for short or sparse vegetation cover, where the ground surface is made visible by the radar.

If we assume that the volume scatterers provide nearly isotropic scattering to the incidence radiation so that σ_2 approximately equals σ_1, we have

$$\sigma_0 \cong \sigma_{0\mathrm{surface}} + \sigma_1 \left(1 + \alpha |R|^2\right). \tag{3}$$

Therefore, the HH/VV ratio can be approximated by

$$\frac{HH}{VV} = \frac{\sigma_{1\mathrm{hh}}}{\sigma_{1\mathrm{vv}}} R_{\mathrm{hhvv}}. \tag{4}$$

The first factor on the right-hand side of the equation accounts for the polarized scattering ratio due to the shape of the scatterers (snow grains or vegetation elements), and the second factor R_{hhvv} accounts for the double-bounce scattering effects

$$R_{\mathrm{hhvv}} = \frac{(\sigma_{0\mathrm{surface-hh}}/\sigma_{1\mathrm{hh}}) + 1 + \alpha |R_h|^2}{(\sigma_{0\mathrm{surface-vv}}/\sigma_{1\mathrm{vv}}) + 1 + \alpha |R_v|^2}. \tag{5}$$

If the volume scattering is much larger than the surface scattering, then

$$R_{0\mathrm{hhvv}} = \frac{1 + \alpha |R_h|^2}{1 + \alpha |R_v|^2}. \tag{6}$$

Table V provides the values of R_{hhvv} and $R_{0\mathrm{hhvv}}$ for four cases for $\alpha = 4$ and $\sigma_{0\mathrm{surface-hh}}/\sigma_{1\mathrm{hh}} = \sigma_{0\mathrm{surface-vv}}/\sigma_{1\mathrm{vv}} = 0.5$. For the case of smooth bare-soil surfaces, the double-bounce scattering can enhance the HH/VV ratio by about 0.5 dB (R_{hhvv}) or about 0.7 dB $(R_{0\mathrm{hhvv}})$. Regardless of the impact of ground-surface scattering, the estimation (0.5–0.7 dB) is close to the HH/VV ratio observed in November 2007.

At the presence of snow cover in December 2006, the HH/VV ratio became smaller than that in November 2007 over the entire study site. If the HH/VV ratio was caused by the double-bounce effects in November 2007, the presence of snow cover would reduce the Fresnel reflection coefficients between the snow and ground interface. Comparing cases 1 and 2 in Table V, we find that the HH/VV ratios can reduce by about 0.5 dB due to the presence of dry snow over dry soil.

After December 2006, one of the regions that showed distinct temporal changes of HH/VV ratio is the triangular area with three corners marked by the three little triangles in Figs. 3–6. The area is primarily covered by Aspen trees, and the ground surface was observable by the radar energy. The VV or HV backscatter of this area in November 2007 was stronger than the backscatter from sagebrush and grass pasture to the east of this region but weaker than that from the coniferous forests to the west in the Park Range (orange color in the top panel of Fig. 3). The lower corner of this triangle corresponds to the Muddy Pass (Fig. 2), where the U.S. Highway 40 meets the Colorado State Highway 14, which connects the Muddy Pass and the triangular mark to the northeast (lower panel, Fig. 7). In addition to this triangular region, we can find similar features in the pasture fields in the Yampa River/Oak Creek watersheds and many other areas. The HH/VV ratio within these areas was close to unity in December 2006 and rose over time to reach about 0.5 dB (yellow color) in January and near 1 dB (orange color) in February 2007. Although the data acquired in March 2008 were about one year after February 2007, the spatial features of HH/VV ratio of these two periods were very similar.

The question is, why should the HH/VV ratio increase over winter from December to March, following a decrease from November to December? Here, we consider two possible contributing factors. One is the double-bounce effect, and the other is the depth hoar. If the double-bounce mechanisms (Fig. 8) did play a role, there probably was a growing ice layer in the snowpack. Without the ice layer, the dielectric contrast is 1.5 versus 2.5 between snow and soil surface (Table IV). The presence of ice layer would create a dielectric contrast of 1.5 versus 3.5 between snow and ice. Consequently, the addition of ice layer would increase the Fresnel reflection coefficient for H polarization (Table V). However, if the ice-layer thickness is much less than the radar wavelength, then the ice layer will be transparent and introduce negligible impact to the Fresnel reflection coefficients. If the thickness of ice

TABLE V
EFFECTS OF DOUBLE BOUNCE ARE PROVIDED FOR FOUR CASES. IT IS ASSUMED THAT THE RATIO OF GROUND-SURFACE AND VOLUME SCATTERING TERMS IS 0.5 FOR EITHER H OR V POLARIZATION

Case	Upper medium	Lower medium	ε for upper medium	ε for lower medium	$\|R_h\|^2$	$\|R_v\|^2$	R_{0hhvv} (dB) for α=4	R_{hhvv} (dB) for α=4
1	Air	Dry soil	1	2.4	0.075	0.024	0.74	0.53
2	Dry snow	Dry soil	1.5	2.4	0.02	0.009	0.19	0.13
3	Air	Ice	1	3.5	0.14	0.055	1.0	0.76
4	Dry snow	Ice	1.5	3.5	0.06	0.03	0.4	0.31

layer on the ground and snow interface grew over time, the ice layer would become increasingly more effective to raise the Fresnel reflection coefficients and hence lead to increasing HH/VV ratio.

The other possible contributing factor is the depth hoar, which is expected to grow over winter. The presence of depth hoar is common in relatively thin snowpack, which is likely to have large temperature gradient from top to bottom. Depth hoar consists of large-grained faceted cup-shaped crystals near the ground, and the depth hoar crystals may grow up to 10 mm in diameter, which is comparable to the wavelength (∼20 mm) of POLSCAT radar frequency. The snow grains in the depth hoar consist of weakly bonded facets. Because the H polarization of radar signals is parallel to the facets, the H polarization may have a stronger response to depth hoar than the V polarization. The differing polarization response to depth hoar may therefore result in the increasing HH/VV ratio over time after December. However, the increase of HH/VV ratio in North Park, where the depth hoar was also present in February, was not as significant as that in the triangular region with deciduous trees. The small change of HH/VV ratio in North Park indicates that the depth hoar was probably not the key contributor to the increase of the HH/VV ratio. We suggest further research with improved *in situ* measurements in this region to pinpoint the exact cause of the increasing HH/VV ratio.

The cross-polarized and copolarized backscatter ratio, HV/VV, provided different perspective of vegetation and snowpack (Fig. 9). The HV/VV ratio data from November 2007 showed strong influence of vegetation, particularly the strong cross-polarized response from the areas with coniferous or deciduous forest stands (yellow and orange colors in the top panel of Fig. 9). Also, over part of the Illinois riverbed near 106.2133° W, where there was prominence of willows along the riverbed, the HV/VV ratio was comparable with that of forested areas, clearly separated from the rest of North Park with the sagebrush or grass pasture fields (green color in the November data). In general, the HV/VV ratio image is similar to the HV image in November 2007.

Similar to the HH/VV ratio, the HV/VV ratio was smaller in December 2006 by 1–2 dB than that in November 2007, particularly over several forested areas in the Park Range, Rabbit Ears Range, and Medicine Bow Mountains. Note that both VV and HV had stronger backscatter in December 2006 than in November 2007 (Figs. 3 and 4). The smaller HV/VV ratio in December 2006 suggested that VV had stronger response to snow accumulation than HV over forested areas (top panels in Fig. 9). Continuing the trend into January 2007, the HV/VV ratio remained lower than that in November 2007, although the ratio did increase slightly from December 2006.

From January to February 2007, it seemed that the HV backscatter increased more rapidly than the VV backscatter. The HV/VV ratio in February 2007 was significantly stronger than that in December 2006 and January 2007 and became more similar to the HV/VV ratio in November 2007. There was a critical change after January 2007 regarding the properties of snowpack. The snowpack remained cold and dry at all times before the end of January 2007 when the air temperature was always below the freezing point. Starting from early February 2007, there were a few warm spells, when the air temperature could reach above the freezing point during daytime. During IOP3, the snow surface was frozen at night and in the early morning and could become wet in the afternoon at some locations in North Park and the Yampa River watershed. For IOP3, we started at about 6–7 A.M. local time and finished the flight over the study site before 11 A.M. to avoid wet-snow conditions during flights. The refrozen snowpack often had hard ice crust near the surface and seemed to contribute more to HV than to VV, resulting in an increase in HV/VV ratio after January 2007.

One striking feature is that the HV/VV ratio in February 2007 allows good separation of the forested areas from other types of vegetation covers, while there was no clear distinction in the HV backscatter (Fig. 5). This feature was confirmed by the data acquired in March 2008. In February 2007, the HV backscatter from snowpack was so strong that it is difficult to distinguish the areas with sagebrush and pasture from the forested (coniferous or deciduous) areas in the HV image (Fig. 5). However, the HV/VV ratio image in February 2007 is strikingly similar to the HV image in November 2007 (Fig. 5), when the HV backscatter provided fairly good representation of differing vegetation covers.

IV. CORRELATION WITH *IN SITU* DATA

During the three IOP field campaigns, several "hourglass" (HG) test sites were selected with intensive *in situ* sampling. The size of each HG site was about 500 m × 500 m (Fig. 10). The ground team made snow pits at the center and corners to measure the snow density, SWE, depth, and stratigraphy. The team also sampled the snow depth at about every 10–20 m along four transects configured in the shape of an HG (Fig. 10). Two of the four transects passed through the center to reach opposite corners and two along the edges of each site. The SWE for the HG sites was estimated as the product of the average snow

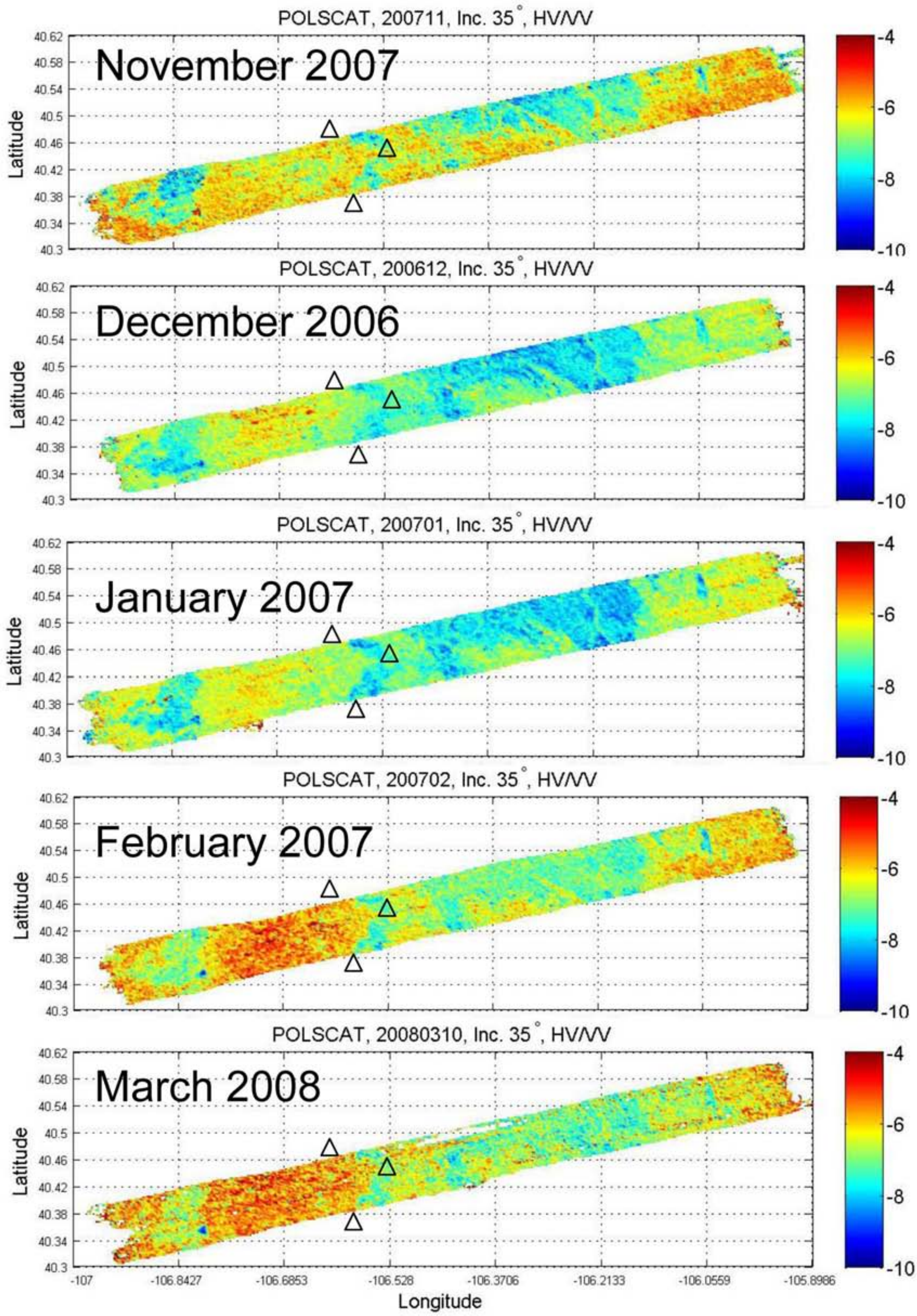

Fig. 9. POLSCAT HV/VV backscatter ratio images from top to bottom are for November 8–9, 2007 (background survey), December 2–5, 2006 (IOP1), January 25–29, 2007 (IOP2), February 22–23, 2007 (IOP3), and March 10, 2008. The HV/VV data are color coded, with the color key in decibels shown in the color bar.

density from the pit data and the average snow depth from transects. Tables VI–VIII provide a summary of the locations of HG sites and the *in situ* measurements acquired during IOP1 and IOP2. The snow depth was about 10 cm in North Park, 20 cm in the Oak Creek sites, and greater than 50 cm in the Rabbit Ears sites in December 2006 and increased by about 20–30 cm from December 2006 to January 2007. In addition, the snow also became more compact with a greater density in January 2007.

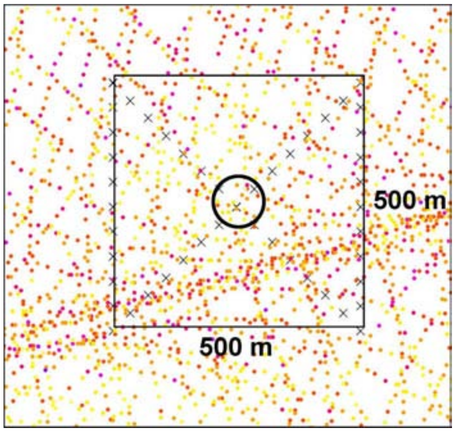

Fig. 10. Dimension of each intensive sampling site is about 500 m $\times$ 500 m. Within the sampling site, the snow depths were measured at many locations in the HG pattern. The small circles represent typical center locations of POLSCAT sampling footprints.

TABLE VI
LOCATION OF INTENSIVE (HG) SAMPLING SITES

Site Name	UTM_E (m)	UTM_N (m)
northpark_deline	398500	4481000
northpark_illinois	395800	4487400
northpark_meyring_east	386940	4485500
Northpark_meyring_west	385000	4485400
oakcreek_brenner	344400	4469500
oakcreek_brown	345883	4474181
oakcreek_catamount	344900	4467900
oakcreek_sydneypeak	343100	4471250
rabbitears_dumontlake	361130	4473760
rabbitears_grand	360400	4476100
Rabbitears_muddycreek_N	361700	4472750
Rabbitears_muddycreek_S	361760	4471100

Currently, there are no instruments that can be used to provide consistent quantitative snow-grain characterization in the field. Therefore, we could only perform qualitative observations of snow-grain characteristics. Snow samples from the pits were put under the microscope in the field. The snow crystals were nominally loosely connected. Shaken lightly, some samples might break into a few snow grains. Under the handheld microscope, we found that the snow grains could have various sizes and irregular shapes. The short and long dimensions were typically in the range of a few millimeters, which agreed with the expected characteristics of snowpack in Colorado.

For each HG site, there were many radar footprints with their centers located within the 500 m $\times$ 500 m box. For example, each dot in the box on the lower right corner of Fig. 12 represents the center of one POLSCAT footprint sampled at about 20-ms interval. For consistent comparison with the averaged SWE data, we included the radar data for averaging only if the center of the radar footprint was within 200 m from the center of the HG sites.

The time series of the VV and HV data are shown in Fig. 11 for several HG sites. The data from November 2007 and March 2008 are shifted by one year to November 2006 and March 2007, respectively, for easier illustration of intraseasonal changes. The data for these sites provide quantitative indications of the temporal change of radar backscatter shown in Figs. 3–6. The data from North Park showed the largest changes, close to 10 dB, from November to March.

The averaged radar data are shown in Fig. 12 against the SWE data from the HG sites for the data acquired from IOP1, IOP2, and November 2007. We do not include the data from February 2007 in the scatter plot because of the significant metamorphism of snowpack due to several melting and refreezing events, which introduced ice lens and crust layers in February. The POLSCAT HH, VV, and HV radar echoes increased by about 0.5-dB/cm SWE for the HG sites in North Park, 0.3 dB/cm in the Oak Creek watershed, and 0.15 dB in the HG sites in the open meadow near the Rabbit Ears peak. The radar response to snow accumulation seemed to be anticorrelated with the backscatter level of the HG sites in November 2007. The Rabbit Ears HG sites had the strongest backscatter (about -17 dB for HV) in November but the smallest backscatter–SWE slope (0.15-dB/cm SWE). The North Park HG sites had the weakest backscatter (about -23 dB for HV) in November but the largest backscatter–SWE slope (0.5-dB/cm SWE). When there was no or little snow in November, the radar backscatter essentially represented the strength of vegetation and ground-surface scattering. If the characteristics of snow do not differ too much between the Rabbit Ears and North Park HG sites, the same amount of snow accumulation will introduce the least change in decibels to the backscatter from the Rabbit Ears HG sites and will produce the most change in decibels to the North Park sites.

Also shown in Fig. 12 are the HH/VV and HV/VV ratios. As discussed before, the HH/VV ratios were generally greater than unity and reached as high as 1 dB for a few sites in North Park and the Oak Creek. The HV/VV ratio, a strong indicator of the vegetation cover, was generally higher for the Rabbit Ears HG sites. The characteristics shown in this figure are consistent with the behavior of polarization ratios shown in Figs. 7 and 9.

V. COMPARISON WITH QuikSCAT DATA

Here, we use the POLSCAT data to study the spatial averaging effects in the coarse-resolution radar observations made by QuikSCAT [19]. QuikSCAT is a spaceborne Ku-band (13.402-GHz) scatterometer designed to measure the normalized radar cross section (σ_0) of sea surfaces for global ocean surface wind mapping. QuikSCAT uses a conical scanning reflector antenna, illuminated by two antenna feed horns to produce two antenna beams. The inner beam operates at a nominal incidence angle of 46° with H polarization, and the outer beam operates at a nominal 54° incidence angle with V polarization. The dimension of the QuikSCAT antenna footprint is about 25 km. The comparative analyses of the QuikSCAT data with the NSA for the data acquired from July 2003 to April 2004 for three sites in Colorado have suggested the presence of snowpack information in Ku-band radar observations for complex landscapes with about 0.1-dB increase per 1-cm change in SWE [15], which is significantly weaker than the POLSCAT observations at a resolution of a few hundred meters.

TABLE VII
IN SITU MEASUREMENTS DURING IOP1

Site Name	Date	Depth_mean (cm)	Depth_stdev (cm)	Density_mean (kg m^3)	Density_stdev (kg m^3)	SWE (mm)
northpark_deline	12/5/2006	11.74	2.57	122.2	18.13	14.4
northpark_illinois	12/4/2006	10.87	5.17	129	16.7	14.0
northpark_meyring_east	12/6/2006	9.24	4.22	174.8	47.07	16.2
northpark_meyring_west	12/5/2006	10.36	3.99	189	47.13	19.6
oakcreek_brenner	12/4/2006	20.77	4.70	161.8	13.77	33.6
oakcreek_brown	12/4/2006	21.49	5.75	171.8	25.97	36.9
oakcreek_catamount	12/4/2006	18.45	2.68	132.2	19.73	24.4
oakcreek_sydneypeak	12/5/2006	20.26	4.77	172.2	28.61	34.9
rabbitears_dumontlake	12/4/2006	58.19	19.98	244.8	10.94	142.5
rabbitears_grand	12/4/2006	85.45	14.73	244.2	15.82	208.7
rabbitears_muddycreek_N	12/5/2006	51.34	13.77	281.4	8.65	144.5
rabbitears_muddycreek_S	12/5/2006	62.51	13.54	232.6	10.81	145.4

TABLE VIII
IN SITU MEASUREMENTS DURING IOP2

Site Name	Date	Depth_mean (cm)	Depth_stdev (cm)	Density_mean (kg m^3)	Density_stdev (kg m^3)	SWE (mm)
northpark_deline	1/26/2007	36.77	7.21	200.2	30.56	73.6
northpark_illinois	1/27/2007	33.23	10.7	198.6	24.14	66.0
northpark_meyring_east	1/26/2007	31.55	16.6	218.6	26.96	69.0
northpark_meyring_west	1/28/2007	29.06	12.8	195.6	45.82	56.8
oakcreek_brenner	1/26/2007	48.89	4.59	171.4	18.68	83.8
oakcreek_brown	1/28/2007	54.88	6.23	189.8	4.82	104.2
oakcreek_catamount	1/27/2007	47.47	3.83	170.4	16.59	80.9
oakcreek_sydneypeak	1/26/2007	49.51	7.3	192.8	10.99	95.5
rabbitears_dumontlake	1/26/2007	92.66	30.03	288.6	20.4	267.4
rabbitears_grand	1/26/2007	111.19	22.53	302.8	18.67	336.7
rabbitears_muddycreek_N	1/27/2007	78.38	17.55	273	35.47	214.0
rabbitears_muddycreek_S	1/25/2007	86.91	15.94	266.6	43.89	231.7

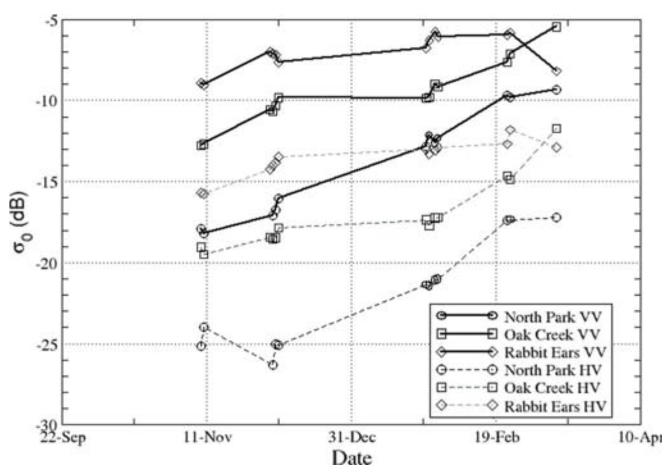

Fig. 11. Time series of POLSCAT VV and HV data near the HG sites, namely, "northpark_deline," "oakcreek_brenner," and "rabbitears_dumontlake." The POLSCAT data are averaged within 200 m from the center of each HG site. The data from November 2007 and March 2008 were shifted back by one year to 2006 and 2007, respectively, to illustrate the change of the backscatter by month.

We selected two locations with distinct vegetation covers in the CLPX-II study site for the comparison of the QuikSCAT data from October 2006 to March 2008 with the POLSCAT data. One location is centered at latitude 40.39° N and longitude 106.6853° W, approximately in the middle of the Park Range dominated by coniferous forests (Fig. 2). The other location is centered at latitude 40.5° N and longitude 106.2133° W in North Park with primarily bare ground or sagebrush. We averaged all the QuikSCAT data with the footprint centers located within 10-km radius from the two selected locations on a daily basis and further separated the QuikSCAT data into morning (A.M.) and afternoon (P.M.) passes. The choice of 10-km-radius circle, rather than a smaller radius, is to obtain a sufficient number of QuikSCAT footprints in the circle to reduce the speckle noise from the average. The nominal random noise of each averaged QuikSCAT data point is about 0.2-dB rms (or about 1-dB peak to peak). The resulting spatial extent of the averaged QuikSCAT data is about 45 km, which is inclusive of the 25-km footprint size and the 20-km diameter for averaging.

The averaged QuikSCAT data for the location centered in the Park Range are shown in Fig. 13. There were no significant differences between the data from A.M. and P.M. passes. Note that the dimension of the integrated QuikSCAT footprint is about 45 km, covering more than just the Park Range, but also part of North Park and the Yampa River/Oak creek watersheds. The time series shows that the QuikSCAT HH and VV backscatters increased by about 2–3 dB from October to late February. Subsequently, there was a drop by 3–4 dB in March, likely due to the melting of snow surface, which

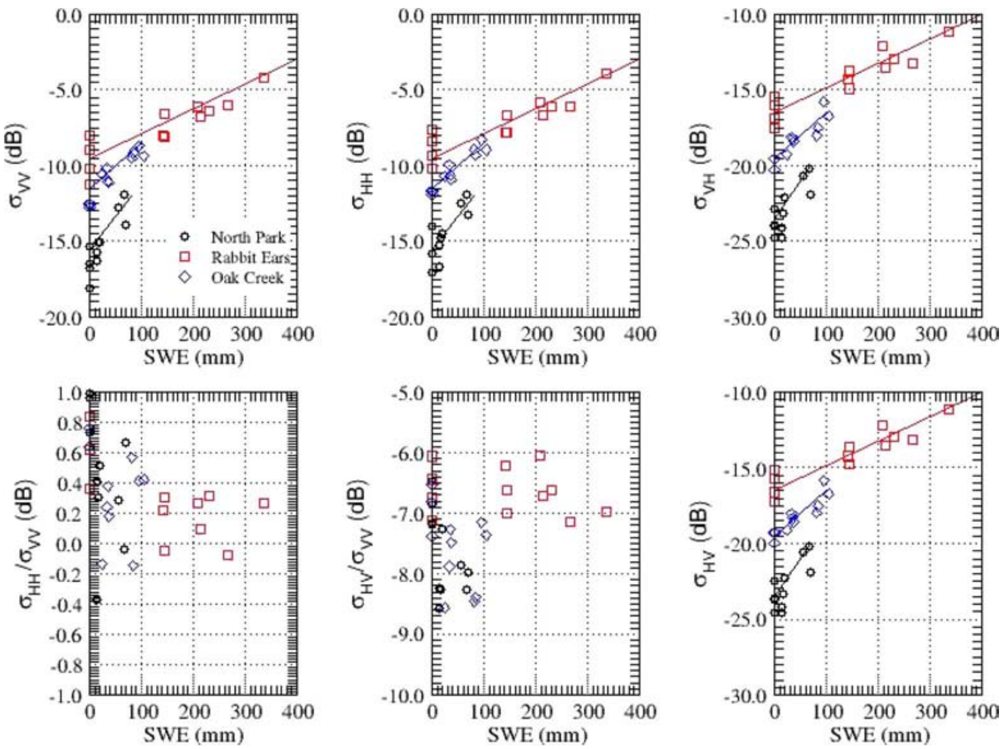

Fig. 12. Comparison of POLSCAT radar data with the snow samples from the HG test sites. The snow depths at several selected test sites were sampled spatially in HG spatial patterns. These test sites are denoted as "HG" sites. Each HG site is about 500 m × 500 m. In addition to snow-depth measurements, snow pits were dug at the center and corners of the test site to sample snow density, grain size, and stratigraphy. The snow-depth measurements were averaged and multiplied by the snow-density observations from the pits to represent the SWE contained in each HG site. The POLSCAT data acquired within 200 m from the center of the HG site were averaged for comparison with the SWE estimate.

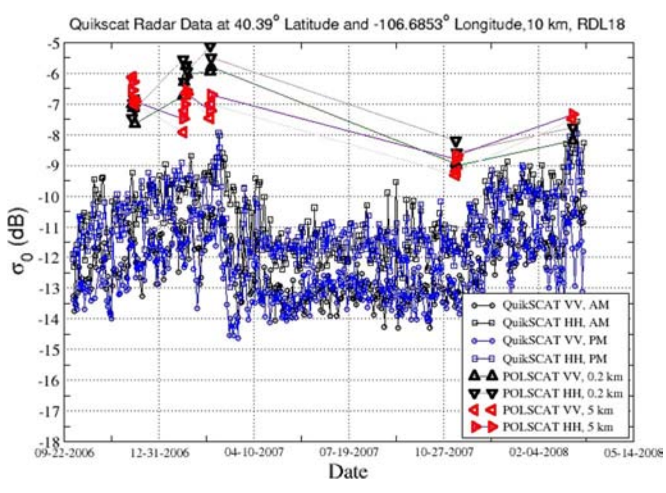

Fig. 13. POLSCAT data near the RDL HG site in the Rabbit Ears Range are compared with the time series of the QuikSCAT data. The upper and lower triangles are for the POLSCAT data averaged within 200 m from the center of the RDL HG site. The left and right triangles indicate the average of the POLSCAT data within 5-km radius. All the QuikSCAT data with footprints located within 10-km radius were averaged to reduce the speckle noise.

reduced the volume scattering from the snowpack. After April, the QuikSCAT backscatter stayed fairly stable from May to late October (Fig. 13).

For comparison with the QuikSCAT data in Fig. 13, we averaged the POLSCAT data if the center of footprint falls within a certain radius from one of the four intensive sampling areas inside the open meadow near the Rabbit Ears peak. This location is indicated by "rabbitears_dumontlake" in Table VI. The POLSCAT data averaged over 200-m radius increased by about 2 dB from December 2006 to February 2007, which seemed to be comparable with the QuikSCAT backscatter changes. However, the POLSCAT data averaged within 5-km radius, including many forest stands and the open meadow, had a small decrease rather than an increasing trend shown in the QuikSCAT data. The decreasing trend of the POLSCAT data averaged over 5-km radius reflected the decrease of radar backscatter from the coniferous forests from December to February (Figs. 3 and 4). This comparison clearly shows that the increase of QuikSCAT data over winter (Fig. 13) was not the result of scattering from the forest stands in the Park Range but essentially was caused by the increase in backscatter from the snow accumulation in the open meadow and the thin snowpack in the Yampa River/Oak Creek watersheds and North Park (Figs. 3–6).

Similar comparison was performed for a selected location in North Park (Fig. 14). The QuikSCAT data showed 2 to 3 dB changes over winter, slightly stronger than the change shown in Fig. 13. Also, the QuikSCAT backscatter in summer for this location is about 1 dB lower than the data centered in the open meadow near the Rabbit Ears Range, where a larger percentage of the area is covered by forest canopies. The POLSCAT data were averaged over an area centered at the point indicated by "northpark_deline" in Table VI. This location in the riverbed of the Illinois River had lower backscatter than the surrounding areas (Fig. 3), and hence, the average of the POLSCAT data within 200-m radius was 3–5 dB lower than that of the QuikSCAT data. Averaging the POLSCAT data within 5-km

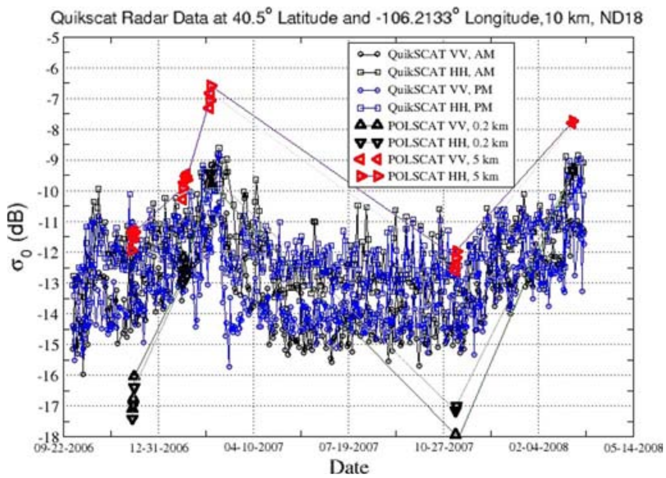

Fig. 14. POLSCAT VV and HH data near the ND HG site in North Park are compared with the time series of the QuikSCAT data. The upper and lower triangles are for the POLSCAT data averaged within 200 m from the center of the ND site. The left and right triangles indicate the average of the POLSCAT data within 5-km radius. All the QuikSCAT data within 10-km radius were averaged to reduce the speckle noise.

radius picks up the stronger backscatter from locations off the riverbed and makes the averaged POLSCAT backscatter more comparable with the QuikSCAT backscatter. The POLSCAT data in North Park showed more significant seasonal transition, i.e., 4 dB for 5-km radius and 7 dB for 200-m radius, than the 3-dB change in the QuikSCAT data. The difference is the result of mixed backscatter from North Park and the surrounding Rocky Mountains in the QuikSCAT data.

The comparisons, shown in Figs. 13 and 14, show the consistencies and differences between the POLSCAT and QuikSCAT data. The high-resolution POLSCAT data present varying response of radar backscatter to terrain covers, while the coarse-resolution QuikSCAT data represent the spatial averaging over mixed vegetation covers and open snowpack.

VI. Summary

The high-resolution Ku-band polarimetric radar data acquired from the CLPX-II in the winter of 2006–2007 and 2007–2008 showed the response of the Ku-band radar echoes to snowpack changes for various types of background vegetation cover. VV and HH backscattering coefficients generally have very similar response to snow accumulation over the study site, although the HH/VV ratio did seem to indicate the effects of double-scattering effects or some other unknown scattering mechanisms. We observed about 0.15–0.5 dB increases in the VV or HH backscatter for every change of 1-cm SWE for dry-snow conditions in December 2006 and January 2007. It appears that more vegetation biomass in the footprint, indicated by stronger radar backscatter in November 2007, resulted in weaker radar response in decibels to SWE. The data in February 2007 and March 2008 showed the impact of depth hoar, ice crust layers, and ice lens growth, which significantly increased the radar backscatter by a few decibels. The results from the campaign support the feasibility of using Ku-band radar for the remote sensing of snowpack.

The data set also shows the critical need to improve the electromagnetic modeling for natural snow cover. The HV backscatter shows significant response to various snowpack in the study site and is also clearly a useful indicator to separate forests from regions with sparse and short vegetation cover. The significant magnitude of HV backscatter is close to 10 dB above the predictions from the traditional dense-media radiative-transfer (DMRT) model for spherical particles [20]. The significant HV observations support the necessity to include nonspherical geometry or multiple-scattering effects in the DMRT model for volume scattering from snow.

Another important driver for modeling improvement is the effect of mixed snow and vegetation in the radar footprint. In the Colorado study site, most regions have short and sparse vegetation, which can cause significant volume scattering and influence the spatial distribution of snow. The behaviors of polarized scattering signals and ratios indicated in the POLSCAT data were probably the result of more than just the individual scattering contributions from snowpack and vegetation but also the interaction between them. We attempted to understand some of the scattering signatures based on very simplified modeling physics, but there is definitely a lack of rigorous analysis to quantify the observed radar signatures, such as the change of HH/VV and HV/VV ratios over time. The POLSCAT/CLPX data point out the need for future modeling research to integrate the vegetation scattering modeling with the snow volume scattering model, such as the DMRT model [17], [20].

The POLSCAT VV or HH response (0.15–0.5-dB/1-cm SWE) seemed to be significantly larger than that indicated by the QuikSCAT and NSA SWE matchup analysis [9], [14], which showed only about 0.1-dB increase for 1-cm-SWE accumulation. Our conclusion is that the QuikSCAT/NSA analysis was influenced by the mixture of forests, sagebrush, pasture, and open snowpack in the coarse-resolution QuikSCAT footprints. The high-resolution data from POLSCAT indicated that the forested areas underwent significantly less or even negative changes in radar backscatter from December to February. The small or negative change of radar backscatter from forests over time is probably the key reason why the QuikSCAT/NSA analysis showed a much smaller response to the change of SWE. We concluded that the positive response of the QuikSCAT data to snow accumulation was essentially contributed by the snow over sagebrush or pasture areas or in the open meadows. To properly apply the QuikSCAT data for snow accumulation analysis, the mixed pixel effects have to be considered, and it is necessary to quantify the temporal change of Ku-band radar backscatter from coniferous forests in the QuikSCAT footprint. We suggest further modeling research and experimental observations for coniferous trees to improve our understanding to help delineate the effects of forest cover in the QuikSCAT data.

Acknowledgment

The work described in this paper that was performed by the Jet Propulsion Laboratory, California Institute of Technology, Pasadena, was carried out under a contract with the National Aeronautics and Space Administration. Also, the work described here included the contributions by the National Operational Hydrologic Remote Sensing Center and the U.S. Forest Service.

REFERENCES

[1] H. Rott, D. Cline, C. Duguay, R. Essery, C. Haas, G. Macelloni, E. Maines, J. Pulliainen, H. Rebhan, and S. Yueh, "CoReH2O—A Ku- and X-band SAR mission for snow and ice monitoring," in *Proc. Eur. Conf. Synthetic Aperture Radar*, Friedrichshafen, Germany, 2008.

[2] R. A. Anthes and B. Moore, III, *Earth Science and Applications From Space: National Imperatives for the Next Decade and Beyond*. Washington, DC: Space Studies Board, Nat. Res. Council, 2007.

[3] J. Dozier, "Remote sensing of the Alpine snow cover: A review of techniques and accomplishments from the visible wavelengths through the microwave," in *Proc. Int. Conf. Snow Hydrol.—CRREL Special Report 98-10,* J. Hardy, M. Albert, and P. Marsh, Eds., Brownsville, VT, Oct. 6–9, 1998, p. 33.

[4] W. H. Stiles and F. T. Ulaby, "The active and passive microwave response to snow parameters. 1. Wetness," *J. Geophys. Res.*, vol. 85, no. C2, pp. 1037–1044, 1980.

[5] F. T. Ulaby and W. H. Stiles, "The active and passive microwave response to snow parameters. 2. Water equivalent of dry snow," *J. Geophys. Res.*, vol. 85, no. C2, pp. 1045–1049, 1980.

[6] F. T. Ulaby, W. H. Stiles, and M. Abdelrazik, "Snowcover influence on backscattering from terrain," *IEEE Trans. Geosci. Remote Sens.*, vol. GRS-22, no. 2, pp. 126–133, Mar. 1984.

[7] T. Strozzi, A. Wiesmann, and C. Mätzler, "Active microwave signatures of snowcovers at 5.3 and 35 GHz," *Radio Sci.*, vol. 32, no. 29, pp. 479–495, 1997.

[8] T. Strozzi and C. Mätzler, "Backscattering measurements of Alpine snowcovers at 5.3 and 35 GHz," *IEEE Trans. Geosci. Remote Sens.*, vol. 36, no. 3, pp. 838–848, May 1998.

[9] J. R. Kendra, S. Sarabandi, and F. T. Ulaby, "Radar measurements of snow: Experiment and analysis," *IEEE Trans. Geosci. Remote Sens.*, vol. 36, no. 3, pp. 864–879, May 1998.

[10] J. Shi and J. Dozier, "Estimation of snow water equivalence using SIR-C/X-SAR. I. Inferring snow density and subsurface properties," *IEEE Trans. Geosci. Remote Sens.*, vol. 38, no. 6, pp. 2465–2474, Nov. 2000.

[11] J. Shi and J. Dozier, "Estimation of snow water equivalence using SIR-C/X-SAR. II. Inferring snow depth and particle size," *IEEE Trans. Geosci. Remote Sens.*, vol. 38, no. 6, pp. 2475–2488, Nov. 2000.

[12] J. Shi, "Estimation of snow water equivalence with two Ku-band dual polarization radar," in *Proc. IGARSS*, 2004, pp. 1649–1652.

[13] J. Shi, "Snow water equivalence retrieval using X and Ku band dual-polarization radar," in *Proc. IGARSS*, Denver, CO, 2006, pp. 2183–2185.

[14] S. V. Nghiem and W.-Y. Tsai, "Global snow monitoring with Ku-band scatterometer," *IEEE Trans. Geosci. Remote Sens.*, vol. 39, no. 10, pp. 2118–2134, Oct. 2001.

[15] D. Cline, S. H. Yueh, S. V. Nghiem, and K. McDonald, "Ku-band radar response to terrestrial snow properties," *EOS Trans. AGU*, vol. 85, no. 47, 2004. Fall Meet. Suppl., Abs. H23D-1149.

[16] D. Cline, K. Elder, S. Yueh, J. Entin, H. Rott, and T. Nagler, "Overview of the second Cold Land Processes Experiment (CLPX-II)," in *Proc. IEEE Int. Geosci. Remote Sens. Symp.*, Barcelona, Spain, 2007.

[17] K.-K. Tse, L. Tsang, C. H. Chan, K. H. Ding, and K. W. Leung, "Multiple scattering of waves by dense random distributions of sticky particles for applications in microwave scattering by terrestrial snow," *Radio Sci.*, vol. 42, no. 5, p. RS5 001, Sep. 2007. DOI:10.1029/2006RS003476.

[18] S. H. Yueh, W. J. Wilson, and S. Dinardo, "Polarimetric radar remote sensing of ocean surface wind," *IEEE Trans. Geosci. Remote Sens.*, vol. 40, no. 4, pp. 793–800, Apr. 2002.

[19] M. W. Spencer, C. Wu, and D. G. Long, "Improved resolution backscatter measurements with the SeaWinds pencil-beam scatterometer," *IEEE Trans. Geosci. Remote Sens.*, vol. 38, no. 1, pp. 89–104, Jan. 2000.

[20] K. H. Ding and L. Tsang, "Effective propagation constants in media with densely distributed dielectric particles of multiple sizes and permittivities," in *Proc. PIER 01*, 1989, pp. 241–295.

[21] C. Mätzler, "Applications of the interaction of microwaves with the natural snow cover," *Remote Sens. Rev.*, vol. 2, p. 287, 1987.

[22] C. Mätzler, "Microwave permittivity of dry snow," *IEEE Trans. Geosci. Remote Sens.*, vol. 34, no. 2, pp. 573–581, Mar. 1996.

[23] S. H. Yueh, B. Stiles, and W. T. Liu, "QuikSCAT wind retrievals for tropical cyclones," *IEEE Trans. Geosci. Remote Sens.*, vol. 41, no. 11, pt. 1, pp. 2616–2628, Nov. 2003.

Simon H. Yueh (M'92–SM'01–F'09) received the Ph.D. degree in electrical engineering from the Massachusetts Institute of Technology, Cambridge, in 1991.

He was a Postdoctoral Research Associate with the Massachusetts Institute of Technology from February to August 1991. In September 1991, he joined the Radar Science and Engineering Section, Jet Propulsion Laboratory, California Institute of Technology, Pasadena. He was the Supervisor of the Radar System Engineering and Algorithm Development Group from 2002 to 2007. He became the Deputy Manager of the Climate, Oceans, and Solid Earth Science Section in July 2007 and was promoted as Section Manager in March 2009. He is also serving as the Instrument Scientist for the National Aeronautics and Space Administration (NASA) Aquarius mission for global sea surface salinity observations. He has been the Principal/Co-Investigator of numerous research projects, including polarimetric wind radiometer research, the airborne scatterometer project for hurricane wind measurements, the Passive/Active L-band Sensor (PALS) project, the NASA Instrument Incubator Project for a mission concept using a large mesh-deployable antenna for soil moisture and ocean salinity sensing, the airborne polarimetric radar (POLSCAT) for ocean wind velocity measurements, the POLSCAT/Cold Land Processes Experiments (CLPX-I and CLPX-II) in 2002–2004 and 2006–2008, the Advanced Component Technology lightweight dual-frequency antenna feed project, and the Aquarius PALS High Wind Campaign in 2009. He is leading the development of Snow and Cold Land Processes mission concept at JPL. He has authored four book chapters and published more than 150 publications and presentations.

Dr. Yueh received the 2002 IEEE Geoscience and Remote Sensing Society (GRSS) Transaction Prize Paper Award, the 2000 Best Paper Award in the IEEE International Geoscience and Remote Symposium, and the 1995 IEEE GRSS Transaction Prize Paper Award for a paper on polarimetric radiometry. He received the JPL Lew Allen Award in 1998 and the Ed Stone Award in 2003.

Steve J. Dinardo received the B.S.E.E. degree from California State University, Los Angeles, in 1983.

In 1978, he joined the Jet Propulsion Laboratory (JPL), California Institute of Technology, Pasadena. At JPL, he has been involved in various projects, including very long base interferometry (VLBI), mobile VLBI, orbiting VLBI, GPS receiver development, and international GPS service. From 1995 to 1997, he was responsible for the deployment of the JPL aircraft polarimetric wind radiometers (WINDRAD) on the National Aeronautics and Space Administration's (NASA) DC-8 and P-3. He successfully coordinated the Hurricane Ocean Wind Experiment, sponsored by NASA and the National Polar-orbiting Operational Environmental Satellite System, resulting in the first airborne Ku-band scatterometer and multifrequency polarimetric radiometer flights over hurricanes. He has also been responsible for the development and deployment of JPL's aircraft rain radar and a 94-GHz cloud profiling radar on NASA's DC-8. He built the JPL Ku-band POLSCAT, deployed on the NCAR C-130, for the first successful demonstration of a polarimetric wind scatterometer technique. He has been responsible for the deployment of POLSCAT and WINDRAD on the Twin Otter, DC-8, and P-3 to support the NASA Cold Land Process Experiments. He is currently involved in the development of low-noise microwave radiometers and radar systems for aircraft and spacecraft for remote sensing of soil moisture and ocean salinity.

Ahmed Akgiray received the B.S. degree (with honors) in electrical engineering from Cornell University, Ithaca, NY, in 2005 and the M.S. degree in electrical engineering from the University of Illinois, Urbana, in 2007, with a thesis entitled "Calibration of Jicamarca Radar Using F-region Incoherent Scatter For Measurements of D-Region Backscatter RCS."

He then joined the Jet Propulsion Laboratory, California Institute of Technology, Pasadena, CA, where he has been working since May 2007. His responsibilities included being a Radar/Radiometer Data Processing and Hardware Engineer for the landing radar of the Mars Science Laboratory (due to be launched in 2011). He is currently working on Soil Moisture Active and Passive satellite RF hardware development.

Richard West received the Ph.D. degree in electrical engineering from the University of Washington, Seattle, in 1994. His Ph.D. thesis applied dense-medium scattering theory to the analysis of passive microwave measurements of Antarctic snow.

In 1995, he started working in the Radar Science and Engineering Section, Jet Propulsion Laboratory, California Institute of Technology, Pasadena. He has worked on the development of algorithms for the processing and calibration of data from the National Aeronautics and Space Administration Scatterometer and from SeaWinds on QuikScat. In 1999, he began working with the radar instrument on the Cassini Mission to Saturn and became the Deputy Task Manager in 2002. From 2002 to 2004, he coordinated a small team that developed software for radar sequence generation and data processing. During the Cassini Prime Mission from 2004 to 2008, he worked on all aspects of instrument operations, including planning the science observations in coordination with the science team, designing the radar command sequences, and processing/calibrating the data received. His research interests include electromagnetic scattering theory, the applications of active and passive microwave data to problems in remote sensing and planetary science, and the development of new techniques/technology to enable more capable remote sensing missions.

Donald W. Cline received the B.A., M.A., and Ph.D. degrees in geography from the University of Colorado, Boulder, in 1989, 1992, and 1995, respectively.

He completed postdoctoral positions with the Department of Hydrology and Water Resources, University of Arizona, Tucson; the School for Environmental Science and Management, University of California, Santa Barbara; and the Institute for Arctic and Alpine Research, University of Colorado. Since 1998, he has been with the National Oceanic and Atmospheric Administration, Chanhassen, MN, where he is the Director of the National Operational Hydrologic Remote Sensing Center, National Weather Service. He has developed and taught courses in surface water hydrology, snow hydrology, geographic information systems, and remote sensing. His scientific and technical interests include hydrologic remote sensing, hydrological modeling, geospatial terrain analysis, cryospheric science, and water resources.

Dr. Cline is a member of the American Geophysical Union.

Kelly Elder received the Ph.D. degree from the University of California, Santa Barbara, in 1995.

He taught hydrology and snow hydrology at Colorado State University, Fort Collins, from 1995 to 2000. In 2000, he joined the Rocky Mountain Research Station, U.S. Department of Agriculture Forest Service, Fort Collins, where he has been a Research Hydrologist since 2000 and has also served as a Project Leader. He is the Scientist-in-Charge at the Fraser Experimental Forest, Fraser, CO. His research interests include snow processes, disturbance hydrology, climate, and avalanches.